International Symposium
On Turbulence and Shear Flow
Phenomena (TSFP-8)
August 28 - 30, 2013 Poitiers, France

EXPERIMENTAL STUDY OF REPRODUCIBILITY OF INSTANTANEOUS STRUCTURE OF THE DETERMINISTIC WALL TURBULENCE

V.I. Borodulin
Institute of Theoretical and Applied Mechanics of Siberian Branch
of the Russian Academy of Sciences, Institutskaya street 4/1,
Novosibirsk, 630090, Russian Federation
Email: Bo@itam.nsc.ru

Y.S. Kachanov
Institute of Theoretical and Applied Mechanics of Siberian Branch
of the Russian Academy of Sciences, Institutskaya street 4/1,
Novosibirsk, 630090, Russian Federation
Email: kachanov@itam.nsc.ru

ABSTRACT

The recently introduced term of 'the deterministic turbulence' refers to the post-transitional boundary-layer flow, which looks like a turbulent one (according to a common viewpoint, thought that viewpoint is not well defined) but displays a noticeable degree of determinism. Such kind of turbulence may occur in boundary layers where transition is caused by instabilities of convective type. The experimental realization of deterministic turbulence has been demonstrated not long ago. The present work deals with analysis of flow structures obtained experimentally in the 2D boundary layer with moderately unfavourable pressure gradient. The vortical structures typical for the turbulent boundary layer were reproduced many times by means of precise reproduction of initial disturbances and maintenance of the mean flow characteristics. Downstream evolution of those typical structures and their increasing divergence within an ensemble of realizations, i.e. the degree of reproducibility of the deterministic turbulence has been documented and analyzed.

INTRODUCTION

There was a common viewpoint on the boundary layer laminar-turbulent transition in the middle and second half of XX century that a phenomenon called the beginning of the flow 'randomization' must occur at a certain late stage of the transition process. It was usually assumed by this term that some random, broadband, and uncontrolled disturbances have to be amplified rapidly and lead to the appearance of stochastic turbulent motions making finally the boundary layer fully turbulent. However, the detailed experimental and numerical studies performed during past decade at more and more controlled disturbance conditions (i.e. at better signal-to-noise ratios) do not result in discovering any clear mechanisms of the final flow randomization. Moreover, the majority of the previously suggested mechanisms of the randomization have been rejected by subsequent, more detailed, investigations (see e.g. papers by Kachanov, 2004; Borodulin et al. 2002 and 2006). That is why the question appeared: "Is it possible that the instantaneous structure of transitional flow would remain deterministic, reproducible and repeatable in the main (at repetition of the same initial conditions) even at super-late, final stages of transition and even in the post-transitional fully turbulent boundary layer?" The affirmative answer to this question was given recently in several studies (see e.g. Borodulin et al., 2007 and 2011).

Similar to the present experiments, those measurements were conducted in a flat plate boundary layer in presence of an adverse pressure gradient. The original laminar base flow was self-similar with constant Hartree parameter equal to −0.115. The laminar-turbulent transition in this boundary layer occurred due to natural development of Tollmien-Schlichting (TS) waves. The uncontrolled background velocity disturbances were kept as low as it was possible, their rms level was less than 0.04% of the free-stream velocity of about 9 m/s (in the frequency range above 1 Hz). The controlled (reproducible) initial disturbances were introduced by means of a special generator. They represented a mixture of a quasi-2D TS-wave (corresponding to the most amplified one) and a broadband 3D disturbance consisted of a wide range of various TS-modes of the frequency-spanwise-wavenumber spectrum. Downstream evolution of those controlled disturbances was natural. It started from the linear-instability amplification region, went through nonlinear stages, and ended with the fully turbulent state of the flow. The post transitional boundary layer was shown to be deterministic, basically. It was possible to reproduce many times the instantaneous velocity field in the turbulent flow. The reproducibility, in turn, provided the possibility of performing detailed quantitative hot-wire measurements in the flow under investigation.

The deterministic turbulence can be regarded as a powerful tool for both applied and fundamental researches. Its first practical application has been demonstrated in Borodulin et al. (2009). In the boundary layer, which was similar to that described above, the instantaneous flow field $U(x, y, z, t)$ was documented in detail in the range of Re = 800 to 1200. Then a Large-

Eddy-Break-Up (LEBU) device was installed at a position with Re = 1050 (x = 500 mm), where the boundary layer was practically fully turbulent, and the instantaneous flow field was documented again. Side-by-side comparison of two instantaneous flow fields allowed us to shed some new light on the physical mechanism of the LEBU device affect on the turbulent boundary layer.

The described above method gives us the unique possibility of experimental comparison of various instantaneous realizations of turbulent flows performed in the present investigation. Such kind of comparison was carried out recently in numerical experiments by Nikitin (2008) and showed some very intriguing results. It was shown that the divergence of turbulent flow fields caused by small difference in initial disturbance conditions can be described by some universal constants. In particular, it was found that the unrepeatable (irreproducible) component of instantaneous velocity fluctuations increases unavoidably in a turbulent channel flow, either with time or with the streamwise coordinate, in an *exponential* way. The increment turned out to be a universal constant, which is independent practically of the problem parameters.

Some of experimental results of examination of the unavoidable increase of irreproducibility of the deterministic turbulent boundary layer obtained in the present experimental study (at conditions similar to those described by Borodulin, 2009 and 2011) are illustrated and discussed below.

EXPERIMENTAL PROCEDURE

The base-flow properties were similar in the present experiments to those studied by Borodulin et al. (2006, 2011). The laminar-turbulent transition and the deterministic turbulence were produced by a superposition of fully controlled 2D and 2D TS-waves. We have carried out and analysed four experiments representing different realizations of the deterministic turbulent boundary layer. They have been named the experiments: *D*, *E*, *EL1*, and *EL2*. Characters *D* and *E* designate two different particular realizations of initial signals excited by the disturbance source, while *L1* and *L2* designate presence in the flow of either LEBU-device #1 of LEBU-device #2, respectively. The two devices represented thin metal plates located parallel to the surface at a distance of 4.2 mm from the wall and having chord lengths of 4 and 8 mm respectively. The LEBU-device trailing edge was always located at x = 500 mm. Every particular realization of the instantaneous flow structure was produced by a particular set of signals many times (up to three hundred thousand times in one set of measurements) by means of a precise reproduction of initial disturbances and maintenance of the mean flow characteristics. Then we have analysed properties of various statistical flow characteristics in different experiments including dependence of irregular (non-reproducible) component of perturbations on the wall-normal, streamwise and spanwise coordinates.

GENERAL EVOLUTION OF DISTURBANCE FIELDS

Figs. 1 to 4 illustrate streamwise evolution of a set of fields (in the (y, z)-plane) of rms intensity of full (total,

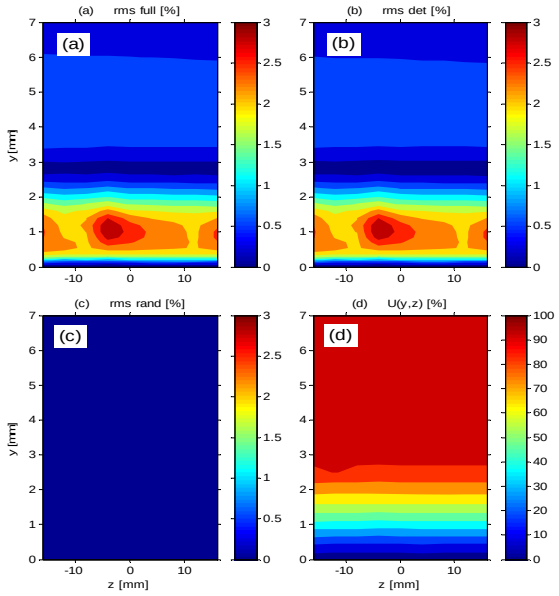

Figure 1. Fields of rms intensity of total (*a*), deterministic (*b*), and random (*c*) components of boundary-layer disturbances measured at "initial" streamwise position x = 350 mm in experiment ***E***. Contours of mean flow velocity are shown in plot (*d*).

A_t), deterministic (A_d), and unreproducible (random, $A_r = A_t - A_d$) components of boundary-layer streamwise-velocity disturbances measured in regime *E* at four successive stages of evolution of the transition process. The fields presented in Figs. 1 and 2 correspond to two stages of boundary-layer transition, while Figs. 3 and 4 are measured in a post-transitional turbulent boundary layer. The corresponding mean-velocity fields are also presented

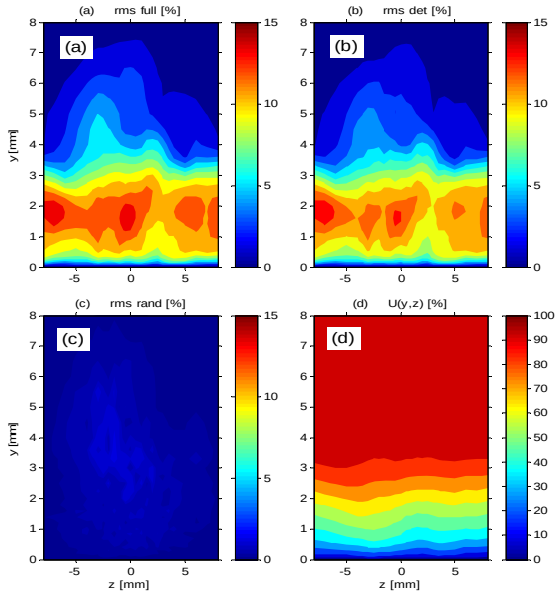

Figure 2. Fields of rms intensity of total (*a*), deterministic (*b*), and random (*c*) components of boundary-layer disturbances measured at late stage of transition (x = 450 mm) in experiment ***E***. Contours of mean flow velocity are shown in plot (*d*).

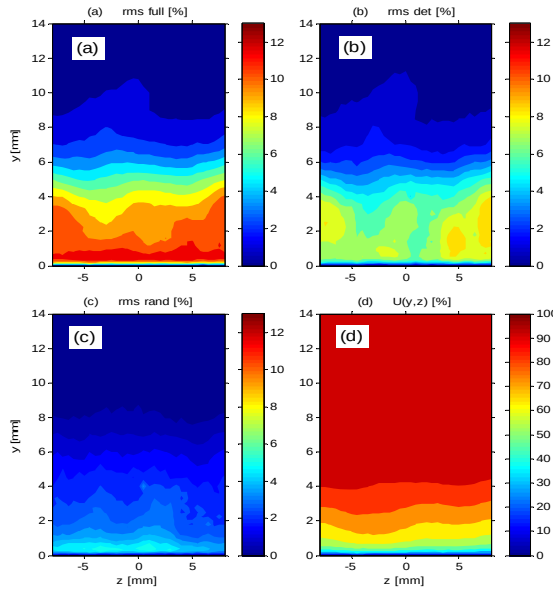

Figure 3. Fields of rms intensity of total (*a*), deterministic (*b*), and random (*c*) components of boundary-layer disturbances measured at stage of just formed deterministic turbulent boundary layer (x = 520 mm) in experiment ***E***. Contours of mean flow velocity are shown in plot (*d*).

in these figures (plots *d*). The results are obtained based on ensemble averaging of 20 velocity time traces having length of 0.183 second each.

It is seen that in the transitional boundary layer (including very late stage shown in Fig. 2), the flow remains very much reproducible; the total (plots *a*) and deterministic (plots *b*) disturbance fields coincide practically with each other, while the unreproducible perturbations (plots *c*) remain very weak at these stages at all values of the spanwise and wall-normal coordinates.

Farther downstream the intensity of random perturbations increases (Figs. 3*c* and 4*c*), especially in the near-wall region, although the deterministic component remains predominant almost in the whole boundary layer.

Qualitatively similar results are observed in other studied regimes. This fact is illustrated in Figs. 5, 6, and 7 displaying results of measurements performed at x = 520 mm in regime *EL1* (i.e. 20 mm downstream from LEBU-device #1) and at x = 550 mm in regimes *EL1* and *EL2* (i.e. 50 mm downstream from LEBU-devices #1 and #2). Note that at x = 520 mm (Fig. 5) the presence of LEBU-device changes very little the fields of all three components of the velocity disturbances. Main distinctions are observed only immediately in the wake of the LEBU-device (around y = 4.2 mm); the reproducibility of the disturbance field is somewhat weaker there. Similar tendencies are seen farther downstream (Figs. 6 and 7), while the influence of the LEBU-devices spreads in the wall-normal direction, especially towards the wall leading to a reduction of the disturbance intensity.

PROPERTIES OF WALL-NORMAL DISTUBANCE PROFILES

Some quantitative information about the wall-normal distributions of rms intensities of the total, deterministic, and random components of the streamwise-velocity perturbations is presented in Figs. 8 to 14 obtained in regime *E* at one of fixed spanwise locations (z = −2 mm) for several streamwise positions (in a range between x = 350 to 590 mm).

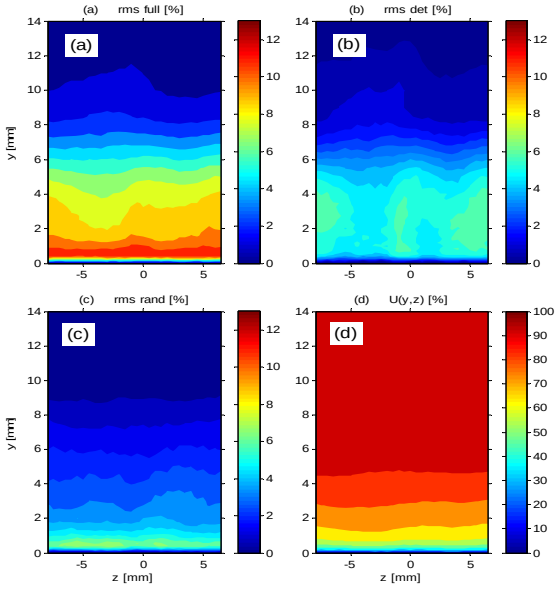

Figure 4. Fields of rms intensity of total (*a*), deterministic (*b*), and random (*c*) components of boundary-layer disturbances measured at stage of developed deterministic turbulent boundary layer (x = 550 mm) in experiment ***E***. Contours of mean flow velocity are shown in plot (*d*).

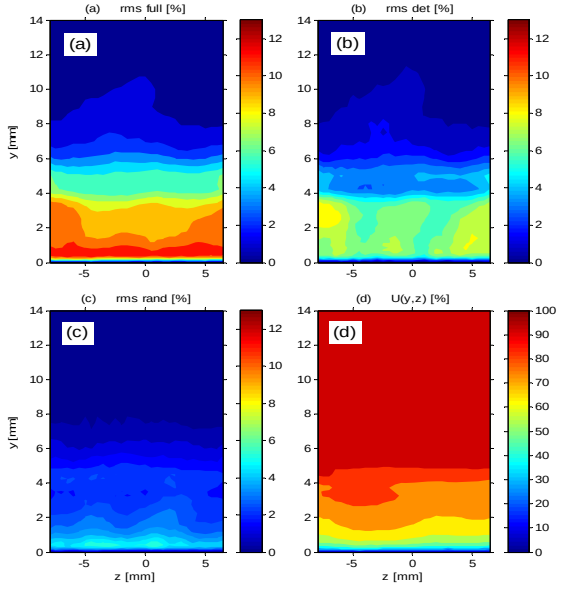

Figure 5. Fields of rms intensity of total (*a*), deterministic (*b*), and random (*c*) components of boundary-layer disturbances measured at stage of just formed deterministic turbulent boundary layer (x = 520 mm) in experiment ***EL1***. Contours of mean flow velocity are shown in plot (*d*).

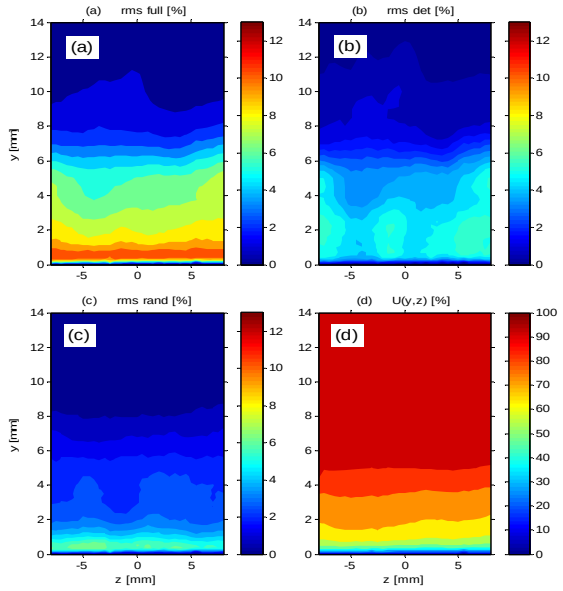

Figure 6. Fields of rms intensity of total (*a*), deterministic (*b*), and random (*c*) components of boundary-layer disturbances measured at stage of developed deterministic turbulent boundary layer (x = 550 mm) in experiment ***EL1***. Contours of mean flow velocity are shown in plot (*d*).

Mean velocity profiles shown in Fig. 8 display that the shape of the profiles evolves gradually from laminar to turbulent one. Starting from streamwise coordinate $x \approx$ 500 mm the shape is stabilized, does not evolve any more and becomes typical for the developed turbulent flow.

The wall-normal profiles of rms intensity of total

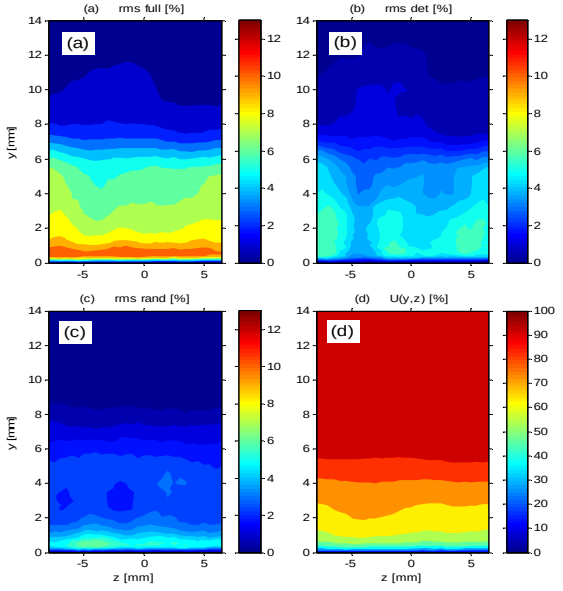

Figure 7. Fields of rms intensity of total (*a*), deterministic (*b*), and random (*c*) components of boundary-layer disturbances measured at stage of developed deterministic turbulent boundary layer (x = 550 mm) in experiment ***EL2***. Contours of mean flow velocity are shown in plot (*d*).

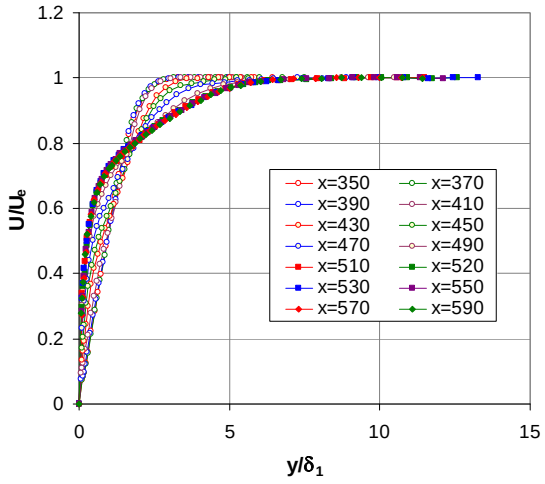

Figure 8. Streamwise evolution of profiles of mean flow velocity measured in experiment ***E*** at $z = -2$ mm.

velocity fluctuations (Fig. 9) evolve from those characteristic for a quasi-2D TS-wave to those typical for the developed turbulent boundary layer. The shape is also stabilized after $x \approx$ 500 mm; further evolution is associated, basically, with a slow reduction of the disturbance intensity. A characteristic strong maximum of fluctuation amplitudes is observed very near the wall and has value of about 12%, that is also very typical for the developed turbulent boundary layers.

The evolution of the shape of wall-normal amplitude profiles of the deterministic (reproducible) component of the streamwise velocity fluctuations is illustrated in Fig. 10 for the same regime *E*. This shape is rather similar to that of the profiles of total velocity fluctuations (shown in Figure 9). The most significant difference is attributed to a smaller magnitude of fluctuations, especially in the near-wall region. The rate of the downstream reduction of amplitude of the deterministic component of fluctuations

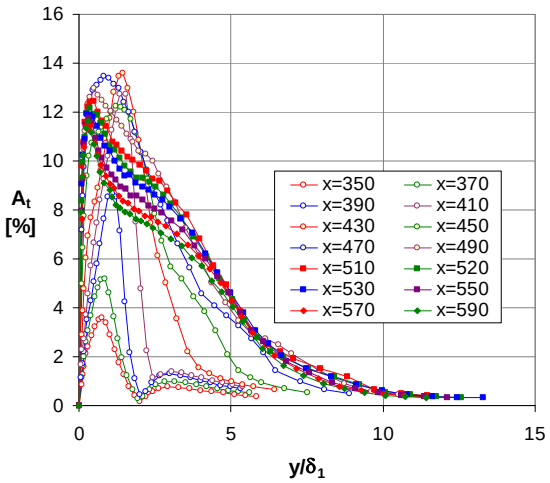

Figure 9. Streamwise evolution of profiles of total rms intensity of flow-velocity fluctuations measured in experiment ***E*** at $z = -2$ mm.

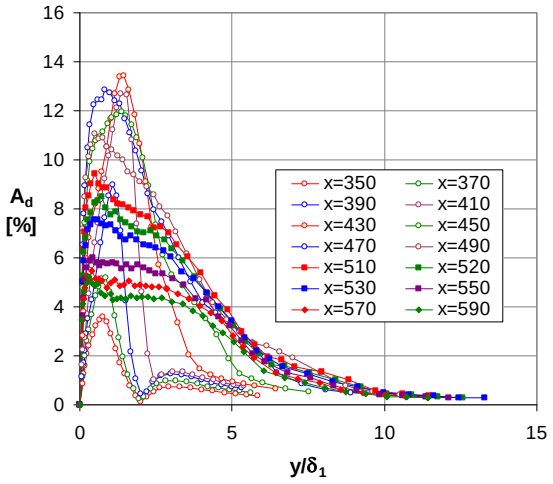

Figure 10. Streamwise evolution of profiles of rms intensity of deterministic (reproducible) component of flow-velocity fluctuations measured in experiment ***E*** at $z = -2$ mm.

is also greater than for the total disturbance.

The corresponding set of wall-normal profiles of the random (unreproducible) component of velocity fluctuations is presented in Fig. 11 (again obtained in regime *E*). Almost in the entire region of boundary-layer transition, including part of late stages (until $x \approx 470$ mm) the largest amplitudes of the random component of velocity perturbations are observed rather far from the wall, between $y \approx 2$ to 3 mm. However, after $x \approx 490$ mm, when the post-transitional turbulent flow appears, the maximum of unreproducible disturbances jumps to the near-wall region and remains there farther downstream. The amplitudes of these uncontrolled perturbations increase gradually downstream.

The relationship between amplitudes of all three kinds

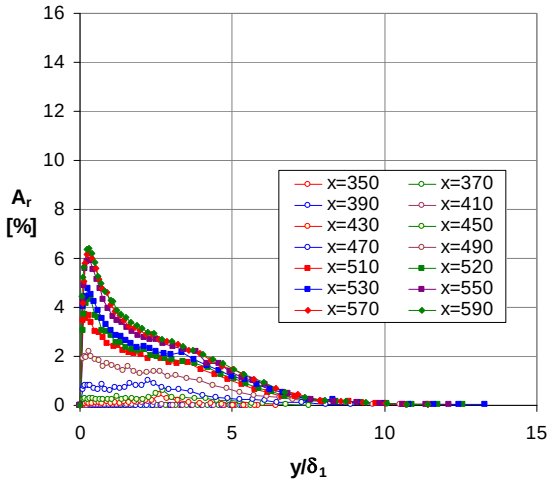

Figure 11. Streamwise evolution of profiles of rms intensity of random (unreproducible) component of flow-velocity fluctuations measured in experiment ***E*** at $z = -2$ mm.

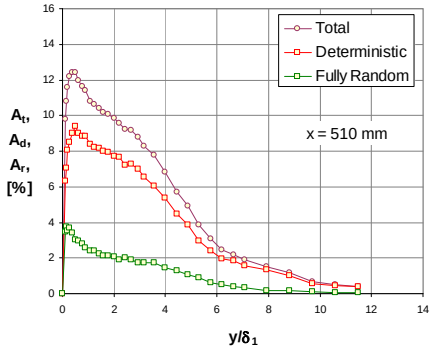

Figure 12. Comparison of wall-normal profiles of rms intensity of three kinds of velocity perturbations: (*i*) total, (*ii*) deterministic, and (*iii*) random measured in experiment ***E*** at $z = -2$ mm, $x = 510$ mm.

of velocity perturbations is illustrated in Figs. 12, 13, and 14 for three successive stages of evolution of post-transitional turbulent boundary layer (at $x = 510$, 520, and 530 mm, respectively). It is seen that the deterministic (reproducible) disturbances are predominant at these stages of flow development, although random (unreproducible) perturbations grow downstream, while the deterministic ones – decay.

The shapes of wall-normal profiles of total and deterministic perturbations are very similar to each other, although the sharpness of the near-wall amplitude peak of the deterministic perturbations gets weaker by $x = 530$ mm compared to that of total disturbances. Meanwhile, the sharpness of the near-wall maximum of profiles of the random (unreproducible) disturbances remains rather strong after $x \approx 500$ mm and the shape of the profiles becomes self-similar (Fig. 15), although somewhat different from that of the total velocity disturbance profiles.

DISTURBANCE AMPLIFICATION CURVES

The amplification curves of rms amplitudes of all three kinds of velocity perturbations are presented in Figs. 16 and 17 for regimes *E* and *D*, respectively. It is seen that

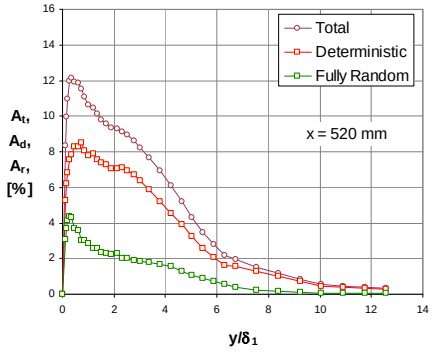

Figure 13. Comparison of wall-normal profiles of rms intensity of three kinds of velocity perturbations: (*i*) total, (*ii*) deterministic, and (*iii*) random measured in experiment ***E*** at $z = -2$ mm, $x = 520$ mm.

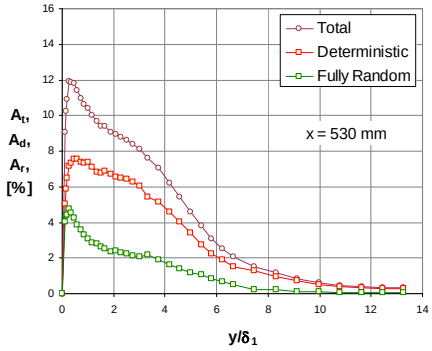

Figure 14. Comparison of wall-normal profiles of rms intensity of three kinds of velocity perturbations: (*i*) total, (*ii*) deterministic, and (*iii*) random measured in experiment ***E*** at $z = -2$ mm, $x = 530$ mm.

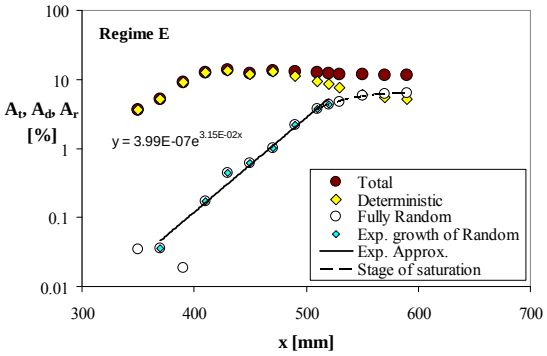

Figure 16. Amplification curves of rms intensity of three kinds of velocity perturbations: (*i*) total, (*ii*) deterministic, and (*iii*) random measured in experiment ***E*** at $z = -2$ mm, $y = y_{max}$ (individual for every mode).

total disturbance amplitude saturates at $x \approx 430$ mm in regime *E* and at $x \approx 470$ mm in regime *D*. Farther downstream it decays slowly in a monotonous way. The amplitude of the deterministic component of perturbations display the same behavior initially but deviate slowly from the total amplitude in the end. The amplitude of random (unreproducible) component of perturbations increase in an exponential way for a long distance and then saturates when it approaches the amplitude of the deterministic component. Note that both the shape of wall-normal profiles and the exponential character of amplification of the unreproducible component of perturbations are in a good agreement with those found in numerical simulation by Nikitin (2008).

This work is supported by the Russian Academy of Sciences.

REFERENCES

Borodulin, V.I., Kachanov, Y.S., and Roschektayev, A.P., 2006, "Turbulence production in an APG-boundary-layer transition induced by randomized perturbations", *Journal of Turbulence*, Vol. 7, N 8, pp. 1-30.

Borodulin, V.I., Kachanov, Y.S., and Roschektayev, A.P. 2007, "The deterministic wall turbulence is possible", *Advances in Turbulence XI. Proceedings of 11th European Turbulence Conference, June 25–28, 2007, Porto, Portugal*, J.M.L.M. Palma and A. Silva Lopes, eds., Springer, Heidelberg, 2007, pp. 176–178.

Borodulin, V.I., Kachanov, Y.S., and Roschektayev, A.P., 2009, "Application of the deterministic turbulence method to study of LEBU-device mechanism", *Advances in Turbulence XII. Proceedings of the 12th EUROMECH European Turbulence Conference*, *Springer Proceedings in Physics*., B. Eckhardt ed., Springer**,** Berlin, Heidelberg, Vol. 132, pp. 313–316.

Borodulin, V.I., Kachanov, Y.S., and Roschektayev, A.P., 2011, "Experimental detection of deterministic turbulence", *J. Turbulence*, Vol. 12, No 23, pp. 1-34.

Kachanov, Y.S., 1994, "Physical mechanisms of laminar-boundary-layer transition", *Ann. Rev. Fluid Mech.*, Vol. 26, pp. 411–482.

Nikitin, N.V., 2008, On the rate of spatial predictability in near-wall turbulence, *J. Fluid Mech.*, V. 614, pp. 495-507.

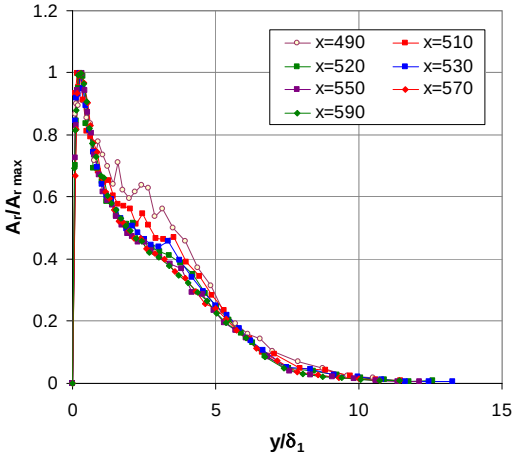

Figure 15. Comparison of wall-normal profiles of rms intensity of three kinds of velocity perturbations: (*i*) total, (*ii*) deterministic, and (*iii*) random measured in experiment ***E*** at $z = -2$ mm, $x = 530$ mm.

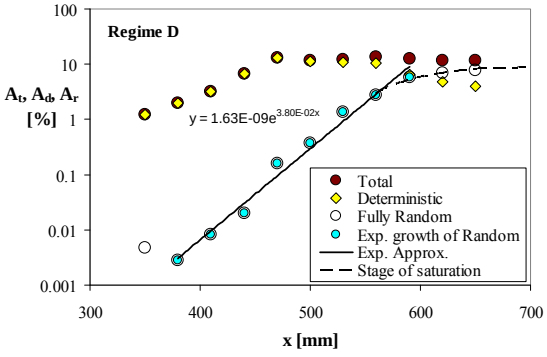

Figure 17. Amplification curves of rms intensity of three kinds of velocity perturbations: (*i*) total, (*ii*) deterministic, and (*iii*) random measured in experiment ***D*** at $z = -8$ mm, $y = y_{max}$ (individual for every mode).